Unusual FTIR and EPR properties of the H_2-activating site of the cytoplasmic NAD-reducing hydrogenase from *Ralstonia eutropha*

Randolph P. Happe[a,1], Winfried Roseboom[a], Gabriele Egert[b], Cornelius G. Friedrich[b], Christian Massanz[c], Bärbel Friedrich[c], Simon P.J. Albracht[a,*]

[a] *E.C. Slater Institute, Biochemistry, University of Amsterdam, Plantage Muidergracht 12, NL-1018 TV Amsterdam, The Netherlands*
[b] *Lehrstuhl Technische Mikrobiologie, Universität Dortmund, Emil-Figge-Strasse 66, D-44221 Dortmund, Germany*
[c] *Institut für Biologie/Mikrobiologie, Humboldt-Universität zu Berlin, Chausseestrasse 117, D-10115 Berlin, Germany*

Received 24 November 1999

Edited by Hans Eklund

Abstract Soluble NAD-reducing [NiFe]-hydrogenase (SH) from *Ralstonia eutropha* (formerly *Alcaligenes eutrophus*) has an infrared spectrum with one strong band at 1956 cm^{-1} and four weak bands at 2098, 2088, 2081 and 2071 cm^{-1} in the 2150–1850 cm^{-1} spectral region. Other [NiFe]-hydrogenases only show one strong and two weak bands in this region, attributable to the $NiFe(CN)_2(CO)$ active site. The position of these three bands is highly sensitive to redox changes of the active site. In contrast, reduction of the SH resulted in a shift to lower frequencies of the 2098 cm^{-1} band only. These and other properties prompted us to propose the presence of a $Ni(CN)Fe(CN)_3(CO)$ active site.

Key words: [NiFe]-hydrogenase; Active site; Cyanide; Carbon monoxide; *Ralstonia eutropha*

1. Introduction

Hydrogenases (reaction: $H_2 \Leftrightarrow 2H^+ + 2e^-$) are widespread among microorganisms. Two classes of metal-containing hydrogenases are known: enzymes containing both nickel and iron ([NiFe]-hydrogenases; for review see [1]) and enzymes which only contain iron ([Fe]-hydrogenases; for review see [2]). The active site in [NiFe]-hydrogenases has been characterised as a $NiFe(CN)_2(CO)$ centre by a combination of X-ray diffraction [3–5] and Fourier-transform infrared spectroscopy (FTIR) studies [6–9]. Nickel is coordinated by four Cys thiols, two of which bridge towards Fe. In [Fe]-hydrogenases an Fe–Fe site with CN and CO ligands serves as the active site. Again, a combination of FTIR studies [10,11] and X-ray diffraction data [12,13] served to understand this active site. Considering the recently released data on three different [Fe]-hydrogenases, the present perception of this site is an Fe(CN)(CO)Fe(CN)(CO) core with a 1,3-propanedithiol molecule providing two thiols bridging between the metals, whereas an additional bridging CO can be present as well. The Fe–Fe centre is linked to a nearby [4Fe–4S] cluster (and the protein) via a single Cys thiol.

[NiFe]-hydrogenases minimally consist of two different subunits. The larger one accommodates the active Ni–Fe site, whereas the smaller subunit contains one to three Fe–S clusters. All enzymes contain a [4Fe–4S] cluster close to the active site (proximal cluster), whereas many enzymes harbour two more clusters, in the *Desulfovibrio gigas* enzyme being a second cubane cluster (distal) and a [3Fe–4S] cluster (medial) situated between the two cubanes [3,4].

The facultative lithoautotrophic Knallgas bacterium *Ralstonia eutropha* contains three different [NiFe]-hydrogenases: a membrane-bound hydrogenase [14,15], a soluble, cytoplasmic hydrogenase (SH) which reduces NAD [14] and an enzyme functional in a H_2-sensing, multicomponent regulatory system [11,16].

The SH, the subject of this report, is a heterotetramer (subunits HoxF, HoxH, HoxU and HoxY with molecular masses of 67, 55, 26 and 23 kDa, respectively [17]). It is composed of two functionally different heterodimer complexes which have been separated and characterised [18–20]. The HoxFU dimer constitutes an enzyme module involved in the reduction of NAD and holds one FMN group and several Fe–S clusters. The HoxHY dimer forms the hydrogenase module within the SH. The 'large' HoxH subunit contains all conserved amino acid residues for binding of the Ni–Fe site, whereas the 'small' HoxY subunit is predicted to contain only the proximal [4Fe–4S] cluster. The SH of *R. eutropha* belongs to a subclass of [NiFe]-hydrogenases where the polypeptide of the small subunit ends shortly after the position of the fourth Cys residue coordinating the proximal cluster. Hence, the basic hydrogenase module in this enzyme only contains the Ni–Fe site and the proximal cluster as prosthetic groups.

The catalytic activity of the SH is insensitive to either O_2 or CO [21,22]. Most [NiFe]-hydrogenases are reversibly inactivated by traces of O_2 and are inhibited by CO in a way competitive to H_2. Several CO-sensitive [NiFe]-hydrogenases have been studied in detail and show up to five redox states of the active site with different electron paramagnetic resonance (EPR), FTIR and activity properties [1,23].

In a preliminary observation [10] it was shown that the SH of *R. eutropha* displayed three instead of two infrared bands in the region where other [NiFe]-hydrogenases show stretching frequencies of the two vibrationally coupled, Fe-bound cyanides. In subsequent studies we have consistently found that untreated, highly active SH shows four weak bands in

*Corresponding author. Fax: (31)-20-525 5124.
E-mail: a311siem@chem.uva.nl

[1] Present address: TNO Nutrition and Food Research Institute, P.O. Box 360, NL-3700 AJ Zeist, The Netherlands

Abbreviations: SH, soluble (cytoplasmic) hydrogenase; BV, benzyl viologen; MV, methyl viologen; EPR, electron paramagnetic resonance; FTIR, Fourier-transform infrared spectroscopy; XAS, X-ray absorption spectroscopy; EXAFS, extended X-ray absorption fine structure

PII: S0014-5793(99)01799-8

the CN region. This and some other observations lead us to propose a $Ni(CN)Fe(CN)_3(CO)$ moiety as the active site in SH. The involvement of the two extra CN^- ligands provides a possible explanation for the unusual properties of the enzyme, as well as for its insensitivity toward oxygen and carbon monoxide.

2. Materials and methods

R. eutropha was cultivated heterotrophically at 30°C in a mineral medium as described before [24]. Cells were stored at −70°C. The SH was purified at 4°C in air as described [25] using 50 mM Tris–HCl (pH 8.0), except for the dye affinity column step, which was performed in 50 mM MOPS (pH 6.8). The SH (in 50 mM Tris–HCl buffer, pH 8.0) was stored in liquid nitrogen. The purity of the samples was examined by SDS–gel electrophoresis [26]. Protein concentrations were determined [27] using bovine serum albumin as standard. The Ni content of the used samples, determined by atomic absorption [9], ranged from 0.6 to 0.8 mol Ni/mol, assuming a molecular mass of 172 kDa.

Hydrogenase activities were measured at 30°C in a 2-ml cell with a Clark electrode (type YSI 5331) for polarographic measurement of H_2 [28]. For H_2 consumption measurements with benzyl viologen (BV) as electron acceptor, enzyme was added to a solution of 50 mM Tris–HCl buffer (pH 8.0), 250 μM $Na_2S_2O_4$ (dissolved in Ar-gassed Tris buffer (pH 8.0)) and 40 μM H_2. After an incubation of 5 min the reaction was started by the addition of 4 mM BV (20 μl aerobic solution). H_2 consumption measurements with NAD as electron acceptor were performed as described above with the exception that the reaction was started by the addition of 2.5 mM NAD (10 μl aerobic solution). NADH oxidation activities with $K_3Fe(CN)_6$ as electron acceptor were measured anaerobically at 30°C in a 1-ml quartz cuvette closed with a septum, monitoring the absorption decrease at 420 nm using a Zeiss M4 QIII spectrophotometer ($\varepsilon = 1$ mM^{-1} cm^{-1} for $K_3Fe(CN)_6$ at 420 nm). The reaction mixture contained 1.25 mM NADH, 10 mM glucose, glucose oxidase (60 units) and 5 μl sample, in Ar-saturated Tris buffer. The reaction was started after 5 min of incubation at 30°C, by the addition of 1 mM $K_3Fe(CN)_6$. Samples of isolated SH were found to catalyse BV and NAD reduction with H_2 at specific activities up to 100 and 85 U/mg (1 U = 1 μmol/min), respectively, whereas $K_3Fe(CN)_6$ was reduced with NADH at rates of about 150 U/mg. Before use, H_2 was passed over a palladium catalyst (Degussa, Hanau, Germany; type E236P), and Ar was passed through an Oxisorb cartridge (Messer-Griesheim, Düsseldorf, Germany), to remove residual O_2.

FTIR spectra [9] and EPR measurements [23] were carried out as before. For FTIR the enzyme samples were concentrated to 0.4–1.5 mM.

3. Results and discussion

Aerobic solutions of most [NiFe]-hydrogenases show a $S = 1/2$ EPR signal due to a nickel-based unpaired spin. The enzymes are inactive in this state. With the *Chromatium vinosum* enzyme, reduction at 2°C removes this signal, while the enzyme still remains inactive [29]. Reduction at elevated temperatures leads to activation of the enzyme and then three more redox states of the active site can be detected. The highest concentration of active enzyme in an EPR-detectable state (the Ni_a–C* state; 0.5–0.9 spins/Ni) can be obtained under 1% H_2 [30,31]. The infrared spectra of the $Fe(CN)_2(CO)$ moiety in the several states clearly reflect electron density and other changes at the Fe ion [6–9].

3.1. FTIR properties

We consistently observed that untreated, highly active *R. eutropha* SH shows one large peak at 1956 cm^{-1} and a set of four weak bands at 2098, 2088, 2081 and 2071 cm^{-1} (Fig. 1A) in the 2150–1850 cm^{-1} spectral region. Treatment with

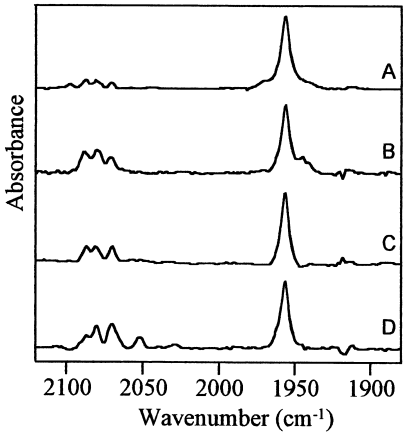

Fig. 1. Infrared spectra of the SH under a variety of redox conditions. A: Untreated, aerobic enzyme. B: Enzyme incubated with 10 mM NADH under Ar (45 min 33°C). C: Enzyme incubated with 10 mM NADH under 100% H_2 (60 min 33°C). D: Enzyme incubated with 5 mM MV under 100% H_2 (60 min 33°C). Spectra are not normalised.

NADH, NADH plus H_2, or H_2 plus methyl viologen (MV) only affected the 2098 cm^{-1} band (Fig. 1). With 10 mM NADH (Fig. 1B), or with 10 mM NADH plus H_2 (Fig. 1C), only the three weak bands at 2088, 2081 and 2071 cm^{-1} were detected, whereas the band at 2098 cm^{-1} disappeared. Slight changes at the base of the strong 1956 cm^{-1} band were detectable as well, but the position of this band did not change. Under reducing conditions in the absence of excess NADH, a fourth band was clearly observed at 2051 cm^{-1} (Fig. 1D). Reduction with dithionite, or dithionite plus MV, produced similar spectra (Fig. 2B,C). Re-oxidation of the sample treated with dithionite plus MV (Fig. 2C), by removal of these agents via gel filtration and subsequent equilibration with air, resulted in the disappearance of the 2051 cm^{-1} band and in the reappearance of the 2098 cm^{-1} band (Fig. 2D). Presently, we do not understand the differences observed in the presence and absence of excess NADH. With H_2 plus substoichiometric amounts of NADH the 2098 cm^{-1} band shifted to 2051 cm^{-1}.

Normal [NiFe]-hydrogenases show only two weak bands in the 2100–2050 cm^{-1} region and one strong band around 1950 cm^{-1}, due to two CN^- and one CO, respectively [7,9], coordinated to Fe in the active site [4]. In analogy, we tentatively assign the four weak bands in the SH spectrum to stretch vibrations of metal-bound CN^- groups, and the strong band to a metal-bound CO. As the strong band and three of the four weak bands did not respond to any of the tested reduction conditions, we assign them to an $Fe(CN)_3(CO)$ moiety which does not undergo any change in coordination or electron density. Since the fourth weak band (2098 cm^{-1}) shifts 47 cm^{-1} to lower frequency upon reduction in the absence of excess NADH, it is unlikely to be due to CN^- bound to the metal ion with the CO ligand; hence we assign it as bound to Ni.

We noticed that in some preparations the H_2–NAD activity and the Ni content of the SH were quite low, although the NADH–ferricyanide activity and the SDS gel pattern (four bands) were as in normal preparations. One such preparation only showed 6% (5.5 U/mg) of the usual specific activity. It also contained only 4% of the amount of Ni expected on the

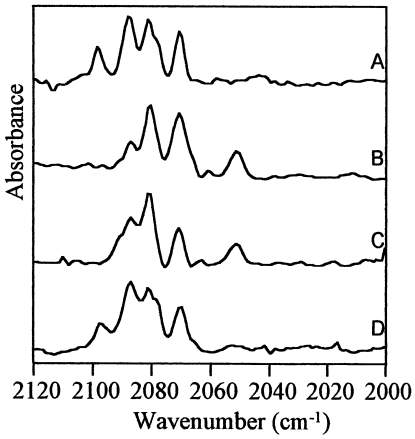

Fig. 2. Infrared spectra of reduced SH in the absence of NADH, and after subsequent reoxidation; only the CN region of the spectra is shown. A: Untreated, aerobic SH (same as Fig. 1A). B: Enzyme incubated with 10 mM dithionite under Ar (60 min 33°C). C: Enzyme incubated with 10 mM dithionite and 5 mM MV under Ar (60 min 33°C). D: As C after removal of dithionite/MV by gel filtration, followed by re-oxidation in air. Spectra are not normalised.

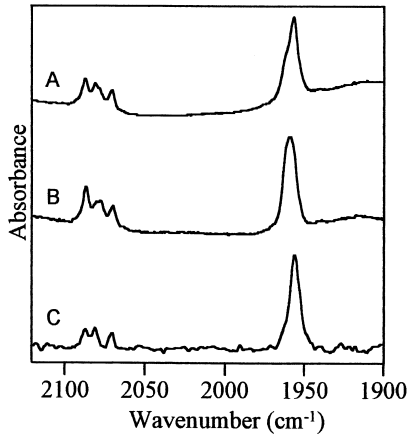

Fig. 3. FTIR spectra of two types of Ni-deficient SH preparations. A: Enzyme (0.8 mM) purified from cells grown in a standard medium. It contained only 4% of the expected amount of Ni and showed a H_2–NAD activity of only 5.5 U/mg (6% of that observed for the best preparations). B: As A, but reduced in the presence of 2 mM deazaflavin and 14 mM EDTA by illumination for 90 min with a 300 W Xe arc. C: Spectrum of purified des-(465–488)-SH (0.78 mM) obtained from cells grown in a standard medium. Spectra are not normalised.

basis of the protein content. Surprisingly, the FTIR spectrum of this preparation (Fig. 3A) was quite intense, but consisted of only four bands: one strong band (1957 cm^{-1}) and three weak bands (2087, 2081 and 2071 cm^{-1}). Maximal reduction of the preparation by illumination in the presence of deazaflavin [11] induced only minute changes in the spectrum (Fig. 3B). When the area of the CO band was compared to the CO bands areas of a fully active SH preparation or of aerobic *C. vinosum* hydrogenase, both of known concentration, then the estimated concentration of the Ni-deficient SH preparation matched the protein-based enzyme concentration rather well. The data are consistent with the presence of only the $Fe(CN)_3(CO)$ moiety. From the fact that the bands occur at positions very close to those of four of the bands observed for intact SH, we tentatively conclude that the vacant Ni site in this preparation is filled with another divalent metal ion, most likely Fe (metal analysis showed Fe and Ni to be the major metals). It further suggests that the presence of the $Fe(CN)_3(CO)$ moiety in the enzyme is apparently not dependent on the presence of a nearby Ni atom. If the three infrared bands are indeed from three CN groups bound to Fe then it can be concluded that the symmetry is low (no three-fold axis). A $K_2[CpFe(CN)_3]$ model compound in methanol shows a rather broad peak at 2025 cm^{-1} with a shoulder at 2014 cm^{-1} and a sharp weaker band at 2053 cm^{-1}; methylation of the cyclopentadienyl (Cp) group shifted all bands 15–17 cm^{-1} to lower frequencies (M.Y. Darensbourg, personal communication). Removal of the three-fold axis is expected to change the spectrum into three, or possibly four, bands [32].

We have observed an FTIR spectrum lacking the 2098 cm^{-1} band also in a purified mutant enzyme (Fig. 3C). Here the Ala-465 in *hoxH*, the gene encoding the large hydrogenase subunit, was replaced by a stop codon resulting in the removal of the C-terminal 24 amino acid long peptide extension, normally present in the precursor form of HoxH. The product, des-(465–488)-HoxH, was shown to be assembled to the tetrameric enzyme by immunoblot experiments [33]. The mutant enzyme, named des-(465–488)-SH, could be purified using the standard procedure used for the SH. It showed no H_2–NAD activity and lacked Ni, although the NADH–ferricyanide activity and EPR spectra of NADH-reduced enzyme were normal (C. Massanz and R.P. Happe, unpublished observations). In this case the intensity of the FTIR bands (at 2087, 2080, 2070 and 1956 cm^{-1}) was only 15% of that expected on the basis of the enzyme concentration (Fig. 3C).

3.2. EPR properties

In untreated, aerobic SH a weak EPR signal (0.1 spin/Ni) was detected at 10 K (sharp peak at $g = 2.02$, broad trough at $g = 1.92$). This has been noted earlier [21] and was ascribed to a $[3Fe–4S]^+$ cluster [22] obtained from the degradation of a 4Fe cluster. We were unable to detect any changes of the signal by incubation under pure O_2 in presence or absence of dyes, treatment with hydrogen-bonding weakening salts, or ferricyanide. Likewise, incubation of the SH with 2-mercaptoethanol or ascorbate plus phenazine methosulphate had no effect on the spectrum. No EPR signals attributable to Ni were observed (4.2–150 K).

Reduction of the SH by H_2 is a very slow process (hours) at room temperature [21,22,34]. In our hands, reduction with H_2 occurred after 45 min at temperatures of at least 30°C. EPR signals of a [2Fe–2S] cluster (1.1 spin/Ni) and a radical ascribed to $FMNH^\bullet$ (0.02 spins/Ni) were detected at 50 K (Fig. 4). Below 10 K additional signals ascribed to reduced cubane clusters were observed (data not shown). Increasing the redox potential by an incubation under Ar or 1% H_2, a procedure used for many [NiFe]-hydrogenases to optimise the Ni_a–C* state [30,31], yielded a sample with a minute Ni_a–C* signal (0.01 spins/Ni), only discernible in dark minus light difference spectra, making use of the light sensitivity of the Ni_a–C* state [35]. The EPR signal of the [2Fe–2S] cluster hardly changed after replacement of 100% H_2 by 1% H_2.

Treatment with H_2 for 45 min at 33°C with subsequent replacement of H_2 by pure O_2 resulted in a spectrum with minor features at $g_{x,y} = 2.31$ and 2.17, resembling those of oxidised enzyme of *C. vinosum* in the ready state

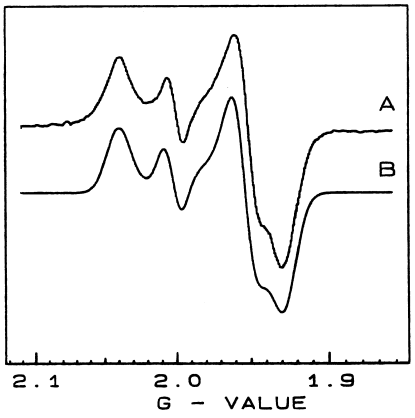

Fig. 4. EPR spectrum of the SH incubated at pH 8.0 under H_2 for 45 min at 33°C, recorded under non-saturating conditions. A: Experimental spectrum. B: Computer simulation of spectrum A as a summation of two signals. Signal I (FMN radical) $g_{x,y,z} = 2.00232$ and widths $(x,y,z) = 2.0735$ mT; signal II ($[2Fe–2S]^+$ cluster) $g_{x,y,z} = 1.92875$ 1.95385, 2.03623 and widths $(x,y,z) = 2.96$, 2.37, 2.75 mT. Simulations of the FMN radical and the [2Fe–2S] cluster were added in a spin–concentration ratio of 1:48, respectively. EPR conditions: microwave frequency, 9416.9 MHz; microwave power incident to the cavity, 2.6 mW; modulation amplitude, 1.27 mT; temperature, 50 K.

($g_{x,y,z} = 2.33$, 2.16, 2.01). The g_z line, expected at $g = 2.02$, was overshadowed by the sharp line of the 3Fe cluster at $g = 2.02$. In *R. eutropha* samples, this nickel signal represented less than 0.01 spin/Ni. So, unlike in other [NiFe]-hydrogenases, the active site remained EPR silent under all redox conditions tested, in agreement with early studies by Schneider et al. [18].

More recently, it has been described that addition of excess NADH in the absence of H_2 resulted in the detection of a significant Ni_a–C* EPR signal (0.3–0.5 spins/molecule [22,36]). In our hands, such conditions did not result in appreciable amounts of Ni_a–C*. We could obtain somewhat stronger Ni_a–C* signals only at pH 6.0 by reduction with 100% H_2 in the presence of 5 mM MV (45 min, 33°C), followed by equilibration under 1% H_2 for 30 min at 20°C (0.24 spins/Ni). At higher pH much less signal was obtained using these conditions (0.06 spins/Ni at pH 9).

3.3. The active site

The data suggest to us that the SH might have a Ni(CN)-$Fe(CN)_3(CO)$ active site bound to four thiols of the four strictly conserved Cys residues in the HoxH subunit (Fig. 5). This would make the Fe site six coordinate and therefore not reactive during the activity cycle of the enzyme. The nickel site would be at least five coordinate. As H_2 cannot readily react with untreated, aerobic enzyme, we assume that the inactive enzyme probably contains an oxygen species occupying the sixth coordination site on Ni. This makes it understandable that removal of the oxygen species (via reduction to water) does not readily occur with H_2, but can be induced rapidly by catalytic amounts of NADH (via the diaphorase module) in the presence of H_2, or with dithionite. We propose that H_2 activation in the SH exclusively takes place on the Ni site. Removal of the oxygen species will also increase the electron density on nickel, thereby shifting the ν(CN) of its bound CN^- to lower frequencies.

The presence of two extra CN ligands in the active site also makes it feasible that the activity of the SH is insensitive towards oxygen and carbon monoxide. The Fe atom cannot be attacked, since its coordination is saturated. The extra CN ligands might impose a serious steric hindrance and might limit access to Ni only to very small molecules (H_2). Indeed we found that the activity assay works equally well in aerobic and in anaerobic buffer. If H_2 is absent and the enzyme is oxidised in air, then the enzyme becomes inactivated again by binding of an oxygen species to nickel.

At this point it is worthwhile to shortly discuss X-ray absorption spectroscopy (XAS) data available for the SH. The structure of the K-edge of nickel in the aerobic, untreated SH, as well as its extended X-ray absorption fine structure (EXAFS) spectrum [37,38], differ considerably from those obtained with other [NiFe]-hydrogenases [37]. The model depicted in Fig. 5 may explain some of the unusual features of the SH. In one study [38] it was concluded from the K-edge of nickel that its coordination number is most likely five or six in the aerobic SH. On bases of X-ray absorption near edge structure and EXAFS spectra a mixed coordination sphere of small and larger donor atoms was proposed (best fit: 4 O at 0.203 nm, 2 S at 0.233 nm and 2 S further away (0.302 nm)). Another study [37] presented similar XAS spectra and likewise concluded that the EXAFS of the untreated SH is dominated by light backscatterers, with contributions from 2–3 S-donor ligands (best fit: 3–4 N or O at 0.206 nm, 2–3 S at 0.235 nm). It must be remembered here that EXAFS cannot distinguish between the light backscatterers C, N or O. The proposed model (Fig. 5) is in line with the presence of 2 small backscatterers (1 C from CN^- and 1 O from a bound oxygen species in inactive, untreated enzyme) on Ni in addition to two bridging and two terminal thiolates.

Reduction of the SH with H_2 in the presence of 0.15 mM NADH [37] induced a conspicuous change in the nickel K-edge, not observable in other enzymes. The resulting spectrum was like that of other [NiFe]-hydrogenases (best fit: 4 S at 0.219 nm). A similar change was observed by Müller et al. [38] after reduction of 1 mM enzyme with 15 or 30 mM NADH under Ar for 10 min at room temperature (best fit: 2 O at 0.206 nm, 3 S at 0.220 nm, 1 S at 0.238 nm). These observa-

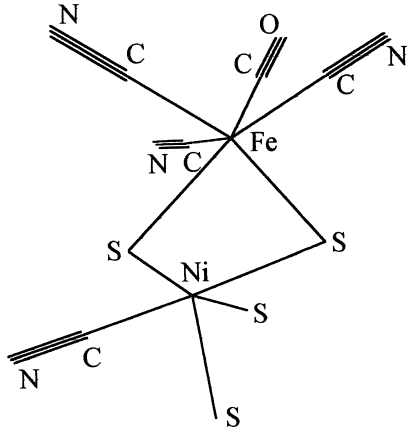

Fig. 5. Schematic representation of the working model of the H_2-activating site in the SH in its active state. The vacant ligand position on the Ni ion is supposed to be the site where H_2 is activated. In untreated, inactive enzyme this site is supposed to hold a bound oxygen species. As a basis for this model, the structure of the Ni–Fe site in normal hydrogenases [3,4] was used.

tions suggest a profound change in the nickel coordination. A difficulty with the SH is that its activity and conformation are apparently very unstable in the reduced state. In an activity assay, virtually all H_2–NAD activity was lost after 10 min at 30°C under H_2 in the presence of NADH [14] and, dependent on the enzyme concentration, the heterotetramer seems to dissociate into two heterodimers [39]. This may have consequences for the stability of the active site. Our preliminary FTIR data on more dilute, reduced SH point to substantial, time-dependent changes of the active site. It is therefore difficult to interpret XAS data of reduced SH without knowledge of the FTIR spectra of the samples used.

Acknowledgements: This work was supported by the Netherlands Foundation for Chemical Research (SON), the Netherlands Organisation for Scientific Research (NWO), the Deutsche Forschungsgemeinschaft, the Bundesministerium für Forschung und Technologie, the Fonds der Chemischen Industrie and the European Union Cooperation in the field of Scientific and Technical Research (COST), Action-818. The authors acknowledge Dr K. Schneider and Prof. A. Müller for their criticism on an early version of the manuscript. We thank Prof. D.J. Stufkens and Mr B. Bleijlevens for advice, and Prof. M.Y. Darensbourg for communicating to us unpublished results on the $K[CpFe(CN)_3]$ compounds.

References

[1] Albracht, S.P.J. (1994) Biochim. Biophys. Acta 1188, 167–204.
[2] Adams, M.W.W. (1990) Biochim. Biophys. Acta 1020, 115–145.
[3] Volbeda, A., Charon, M.-H., Piras, C., Hatchikian, E.C., Frey, M. and Fontecilla-Camps, J.C. (1995) Nature 373, 580–587.
[4] Volbeda, A., Garcin, E., Piras, C., De Lacey, A.I., Fernandez, V.M., Hatchikian, E.C., Frey, M. and Fontecilla-Camps, J.C. (1996) J. Am. Chem. Soc. 118, 12989–12996.
[5] Higuchi, Y., Yagi, T. and Noritake, Y. (1997) Structure 5, 1671–1680.
[6] Bagley, K.A., Duin, E.C., Roseboom, W., Albracht, S.P.J. and Woodruff, W.H. (1995) Biochemistry 34, 5527–5535.
[7] Happe, R.P., Roseboom, W., Pierik, A.J., Albracht, S.P.J. and Bagley, K.A. (1997) Nature 385, 126.
[8] De Lacey, A.L., Hatchikian, E.C., Volbeda, A., Frey, M., Fontecilla-Camps, J.C. and Fernandez, V.M. (1997) J. Am. Chem. Soc. 119, 7181–7189.
[9] Pierik, A.J., Roseboom, W., Happe, R.P., Bagley, K.A. and Albracht, S.P.J. (1999) J. Biol. Chem. 274, 3331–3337.
[10] Van der Spek, T.M., Arendsen, A.F., Happe, R.P., Yun, S., Bagley, K.A., Stufkens, D.J., Hagen, W.R. and Albracht, S.P.J. (1996) Eur. J. Biochem. 237, 629–634.
[11] Pierik, A.J., Hulstein, H., Hagen, W.R. and Albracht, S.P.J. (1998) Eur. J. Biochem 258, 572–578.
[12] Peters, J.W., Lanzilotta, W.N., Lemon, B.J. and Seefeld, L.C. (1998) Science 284, 1853–1858.
[13] Nicolet, Y., Piras, C., Legrand, P., Hatchikian, C.E. and Fontecilla-Camps, J.C. (1999) Structure 7, 12–23.
[14] Schneider, K. and Schlegel, H.G. (1976) Biochim. Biophys. Acta 452, 66–80.
[15] Schink, B. and Schlegel, H.G. (1979) Biochim. Biophys. Acta 567, 315–324.
[16] Lenz, O. and Friedrich, B. (1998) Proc. Natl. Acad. Sci. USA 95, 12474–12479.
[17] Tran-Betcke, A., Warnecke, U., Böcker, C., Zaborosch, C. and Friedrich, B. (1990) J. Bacteriol. 172, 2920–2929.
[18] Schneider, K., Cammack, R. and Schlegel, H.G. (1984) Eur. J. Biochem. 142, 75–84.
[19] Zaborosch, C., Köster, M., Bill, E., Schneider, K., Schlegel, H.G. and Trautwein, A.X. (1995) Biometals 8, 149–162.
[20] Massanz, C., Schmidt, S. and Friedrich, B. (1998) J. Bacteriol. 180, 1023–1027.
[21] Schneider, K., Cammack, R., Schlegel, H.G. and Hall, D.O. (1979) Biochim. Biophys. Acta 578, 445–461.
[22] Erkens, A., Schneider, K. and Müller, A. (1996) J. Biol. Inorg. Chem. 1, 99–110.
[23] Happe, R.P., Roseboom, W. and Albracht, S.P.J. (1999) Eur. J. Biochem. 259, 602–609.
[24] Haverkamp, G.K., Ranke, H. and Friedrich, C.G. (1995) Appl. Microbiol. Biotechnol. 44, 513–518.
[25] Friedrich, C.G., Schneider, K. and Friedrich, B. (1982) J. Bacteriol. 152, 42–48.
[26] Laemmli, U.K. (1970) Nature 227, 680–685.
[27] Bradford, M.M. (1976) Anal. Biochem. 72, 248–254.
[28] Wang, R., Healey, F.P. and Meyers, J. (1971) Plant Physiol. 48, 108–110.
[29] Coremans, J.M.C.C., Van der Zwaan, J.W. and Albracht, S.P.J. (1992) Biochim. Biophys. Acta 1119, 157–168.
[30] Coremans, J.M.C.C., Van Garderen, C.J. and Albracht, S.P.J. (1992) Biochim. Biophys. Acta 1119, 148–156.
[31] Barondeau, D.P., Roberts, L.M. and Lindahl, P.A. (1994) J. Am. Chem. Soc. 116, 3443–3448.
[32] Nakamoto, K. (1997) Infrared and Raman Spectra of Inorganic and Coordinated Compounds, John Wiley and Sons, New York.
[33] Massanz, C., Fernandez, V.M. and Friedrich, B. (1997) Eur. J. Biochem. 245, 441–448.
[34] Schneider, K. and Schlegel, H.G. (1981) Biochem. J. 193, 99–107.
[35] Van der Zwaan, J.W., Albracht, S.P.J., Fontijn, R.D. and Slater, E.C. (1985) FEBS Lett. 179, 271–277.
[36] Gessner, Ch., Trofanchuk, O., Kawagoe, K., Higuchi, Y., Yasuoka, N. and Lubitz, W. (1996) Chem. Phys. Lett. 256, 518–524.
[37] Gu, Z., Dong, J., Allan, C.B., Choudhury, S.B., Franco, R., Moura, J.J.G., Moura, I., LeGall, J., Przybyla, A.E., Roseboom, W., Albracht, S.P.J., Axley, M.J., Scott, R.A. and Maroney, M.J. (1996) J. Am. Chem. Soc. 118, 11155–11165.
[38] Müller, A., Erkens, A., Schneider, K., Müller, A., Nolting, H.-F., Solé, V.A. and Henkel, G. (1997) Angew. Chem. Int. Ed. Engl. 36, 1747–1750.
[39] Keefe, R.G., Axley, M.J. and Harabin, A.L. (1995) Arch. Biochem. Biophys. 317, 449–456.